SUPPORTING METHODS

MicroPET/CT Imaging. Mice were kept warm, under gas anesthesia (2% isoflurane) and injected with 200 μCi of ^{18}F-labeled probes (i.v.). 1 hr interval for uptake was allowed between probe administration and microPET/CT scanning. Data were acquired using a Siemens Preclinical Solutions (Knoxville, TN) microPET Focus 220 and a MicroCAT II CT instrument. MicroPET data were acquired for 10 min and was reconstructed using statistical maximum a posteriori probability algorithms (MAP) into multiple frames (*1*). The spatial resolution of PET is ~1.5 mm, 0.4 mm voxel size. CT images are at low dose 400 μm resolution acquisitions, with 200 μm voxel size. MicroPET and microCT images were co-registered using a previously described method (*2*). 3D regions of interest (ROI) were drawn using AMIDE software (*3*). Color scale is proportional to tissue concentration with red being the highest and lower values in yellow, green & blue.

Production of recombinant CDA and dCK. Human CDA and dCK (plasmids were gifts from Dr. Margaret Black at Washington State University) were expressed in *E. coli*. Protein induction was carried out at 37ºC with 1 mM IPTG (Fisher Scientific) for at least four hours. The cells were lysed via sonication followed by three cycles of freeze-thawing using liquid nitrogen and a 37ºC water bath. Poly-His-tagged proteins were purified using HisPur™ Cobalt Resin (Pierce); purity was checked by SDS-PAGE.

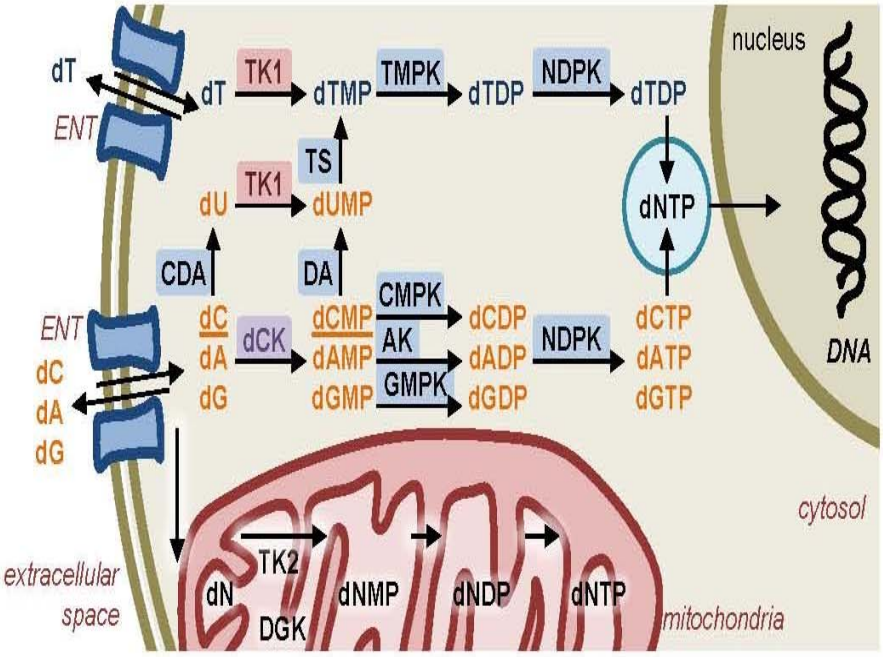

Supplemental Figure 1: dCK regulates a rate-limiting step in the deoxyribonucleoside salvage pathway. dCK is the only salvage enzyme that can supply cells with all 4 precursors of DNA, 3 of them through direct phosphorylation and trapping of dC, dA and dG and the fourth through metabolic processing of dCMP to dTMP. ENT, equilibrative nucleoside transporter; CDA, cytidine deaminase; DA, dCMP deaminase; TS, thymidylate synthase; AK, adenylate kinase; GMPK, guanylate kinase; CMPK, cytidylate kinase; TMPK, thymidylate kinase; NDPK, nucleotide diphosphate kinase.

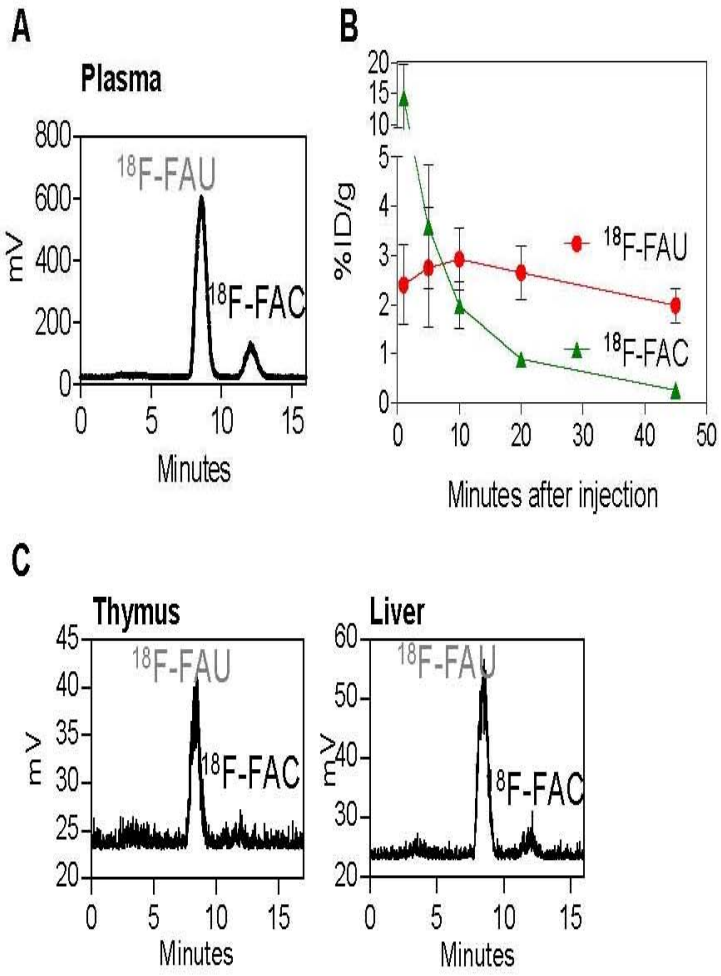

Supplemental Figure 2: *In vivo* metabolite analysis of ^{18}F-FAC. (A) HPLC analysis of plasma samples 45 min following ^{18}F-FAC injection. (B) Plasma clearance rates of ^{18}F-FAC and ^{18}F-FAU analyzed by HPLC (assuming no other radioactive metabolites present in blood); (C) HPLC analysis of the deamination metabolite of ^{18}F-FAC, ^{18}F-FAU, accumulation in thymus and liver. Traces show accumulation of the probes at 45 minutes after i.v. injection of ^{18}F-FAC into C57/BL6 mice. Results are representative of $n \geq 2$ independent experiments.

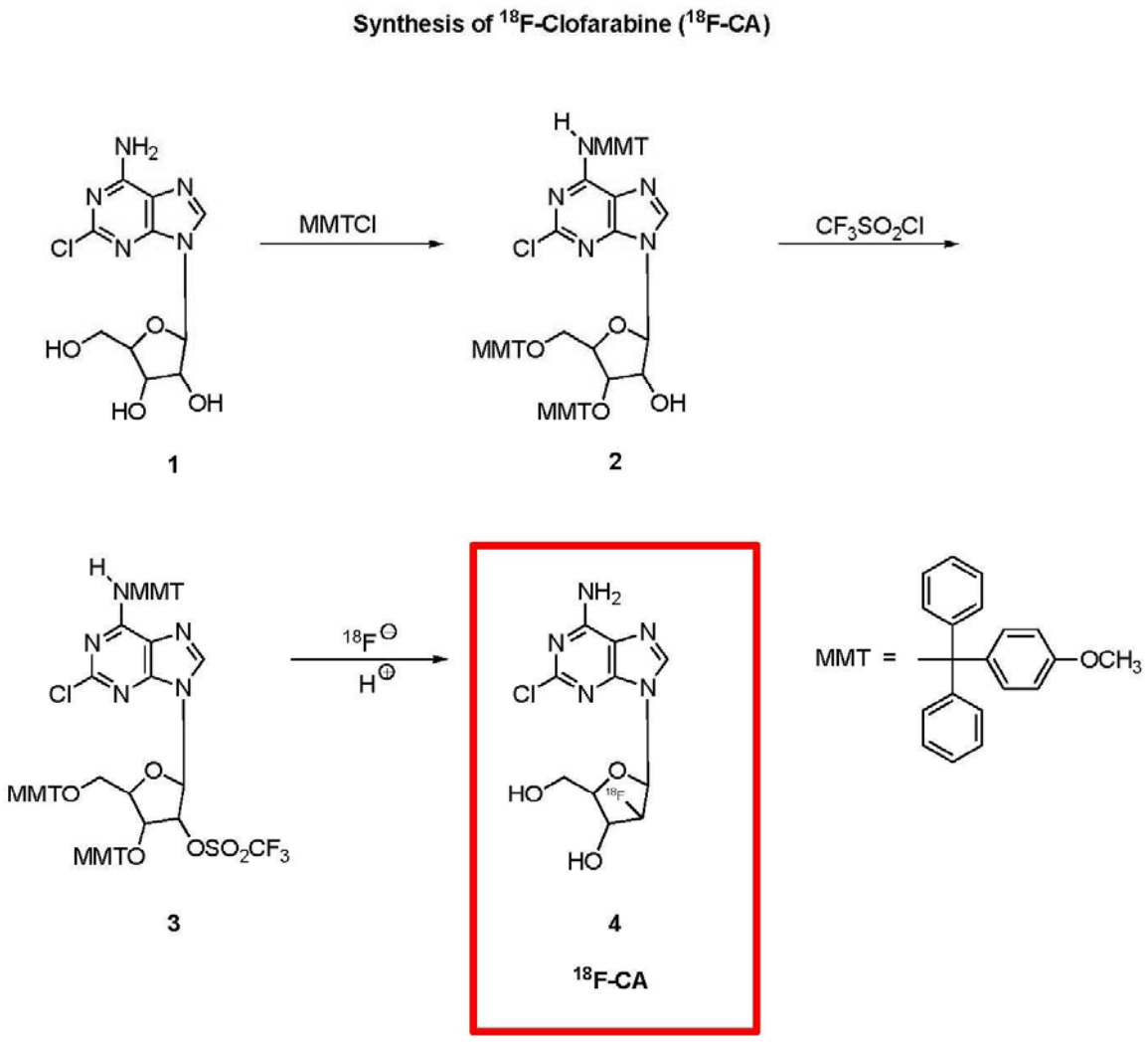

Supplemental Figure 3: Radiochemical synthesis of 2-Chloro-9-(2'-deoxy-2'-^{18}F-beta-D-arabinofuranosyl) adenine – ^{18}F-CA (^{18}F-labeled Clofarabine). The trityl protected chloroadenosine derivative **2** was prepared by a general procedure developed previously (*4*). Thus, 2-chloroadenosine (**1**) (9.2 mmol), 4-dimethylaminopyridine (9.2 mmol) and monomethoxytrityl chloride (32.4 mmol) were placed in a dry 250 mL round bottom flask under argon and 80 mL of dry pyridine was added. The mixture was stirred at 90ºC for 18 hr. Pyridine was evaporated in rotary evaporator and the last traces of it were azeotropically removed with toluene. The residue was dissolved in dichloromethane and washed with water. The organic layer

was dried with Na_2SO_4, filtered and evaporated. The crude product was subjected to silica gel column chromatography with 25% ethyl acetate in hexane as the eluent to isolate pure hydroxy product **2**. The triflate **3** was prepared from the corresponding hydroxy derivative **2** as follows: The hydroxy compound **2** (0.1 mmol) was dissolved in 3 mL of dichloromethane under argon and 4-dimethylaminopyridine (0.18 mmol) was added. The solution was cooled in an ice bath at 0ºC for 10 min. Triflyl chloride (0.02 mL) was then added and the reaction mixture was gradually warmed to room temperature and stirred for 3 hr. The reaction mixture was diluted with 10 mL of dichloromethane and washed with water. The organic layer was dried with Na_2SO_4. Evaporation of dichloromethane gave an oily residue, which was purified by silica gel column chromatography using 30% ethyl acetate in hexane as eluent provided the pure triflate derivative **3**.

No-carrier-added ^{18}F-fluoride ion was produced by 11 MeV proton bombardment of 98% enriched ^{18}O-water in a silver target body using a RDS-112 cyclotron. The aqueous ^{18}F-fluoride ion was treated with a solution of K_2CO_3 (1 mg) and Kryptofix 2.2.2 (10 mg) dissolved in water (0.04 mL) and acetonitrile (0.75 mL) mixture. The solution was evaporated at 115ºC with a stream of nitrogen gas. The residue was dried by the azeotropic distillation with acetonitrile (3 x 0.5 mL). The triflate precursor **3** (10 mg) dissolved in 1 mL of acetonitrile was added to the dried K^{18}F/Kryptofix complex and reacted at 110ºC for 25 min. The reaction mixture was cooled to room temperature and passed through a small cartridge of silica gel. The cartridge was eluted with 4 x 2 mL of ethyl acetate. The ethyl acetate was evaporated to dryness and the residue was then dissolved in 0.5 mL of acetonitrile. One mL of 1M HCl was added to the acetonitrile solution and heated at 100ºC for 5 min. The reaction mixture was diluted to a total volume of 3 mL with a solution of 15% ethanol and 85 % 25 mM ammonium acetate in water and injected into a semi-preparative HPLC column (Phenomenex Gemini C-18 column; 25 x 1 cm) and eluted with a mobile phase of 15% ethanol and 85% 25 mM ammonium acetate in water at a flow rate of 5.0 mL/min. The effluent from the column was monitored with an UV detector (λ = 263 nm) and a gamma radioactive detector. The chemically and radiochemically pure ^{18}F-labeled product **4** with retention time between 11 and 13 min isolated in 10 – 15% radiochemical yield was made isotonic by dilution with sterile saline solution which also decreased the concentration of ethanol to < 10%. The solution was then sterilized by passing through a Millipore sterilizing filter (0.22 μm) into a sterile multi-dose vial.

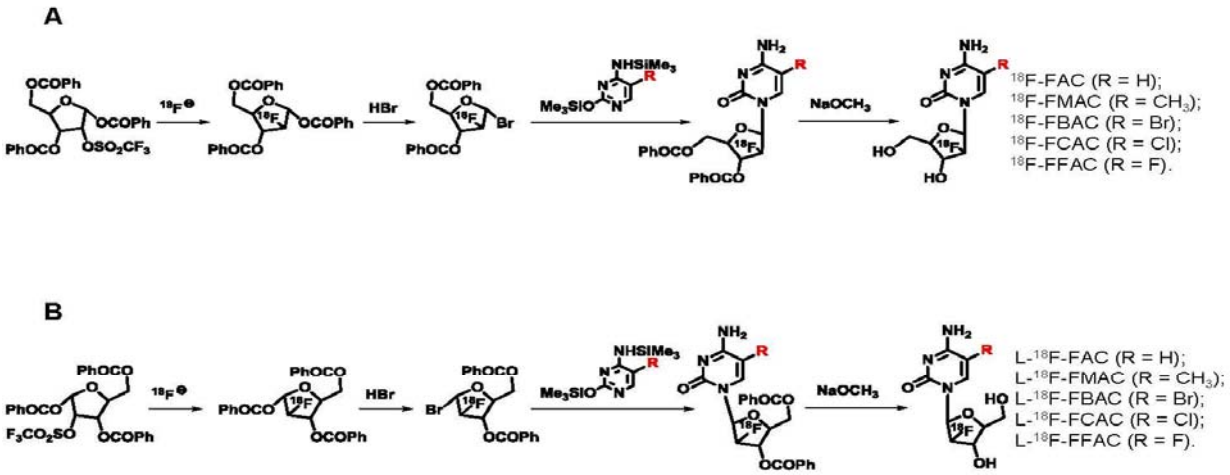

Supplemental Figure 4: Radiochemical synthesis of ^{18}F-labeled D- and L-analogs. The reaction schemes to synthesize these compounds were similar to that previously reported for ^{18}F-FAC synthesis (*5*, *6*). Typical procedures for the syntheses of D-isomers (**A**) and L-isomers (**B**) of ^{18}F-FAC are provided. The synthesis of all the other FAC family of probes utilized the methods outlined herein using the appropriate 5-substituted cytosine silyl analogs.

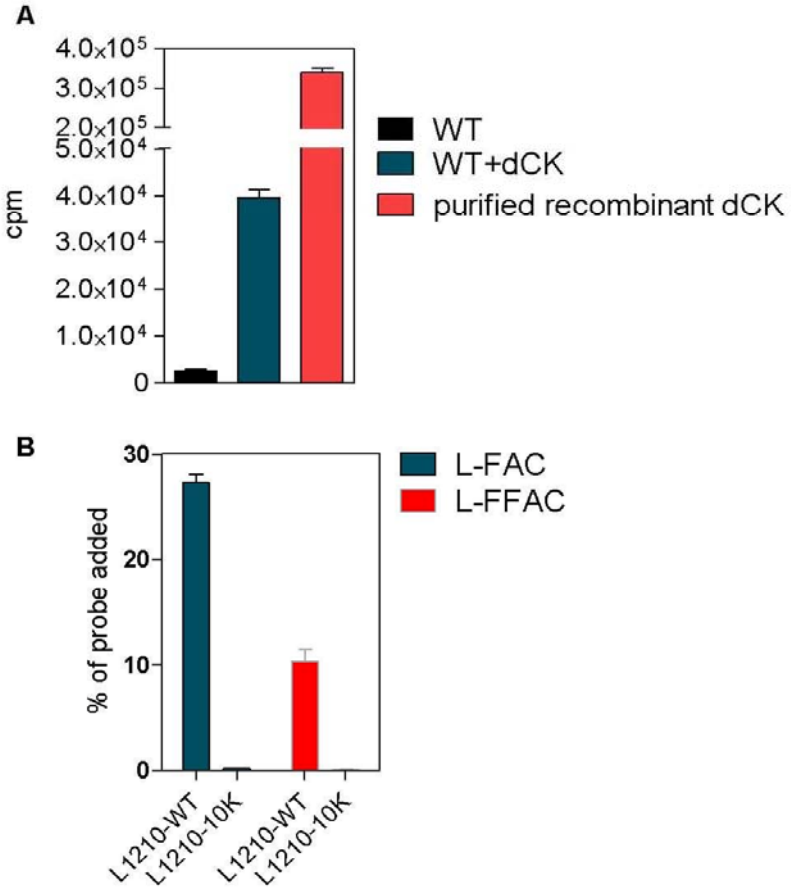

Supplemental Figure 5: **L-^{18}F-FAC and L-^{18}F-FFAC**. To determine if L-FAC was phosphorylated by dCK, a kinase assay was performed with the purified recombinant human dCK and the ^{18}F-labeled L-FAC (**A**). As controls, lysates from wild-type *E. coli* (WT) and *E. coli* induced to overexpress the human protein (WT+dCK) were included. Kinase assays were also performed using lysates from dCK-positive L1210 and dCK-negative L1210-10K cells (**B**) and either L-^{18}F-FAC or L-^{18}F-FFAC. For all the kinase assays shown, 1 µg of total protein was used for each sample. The kinase assays were carried out at 37ºC for 20 minutes.

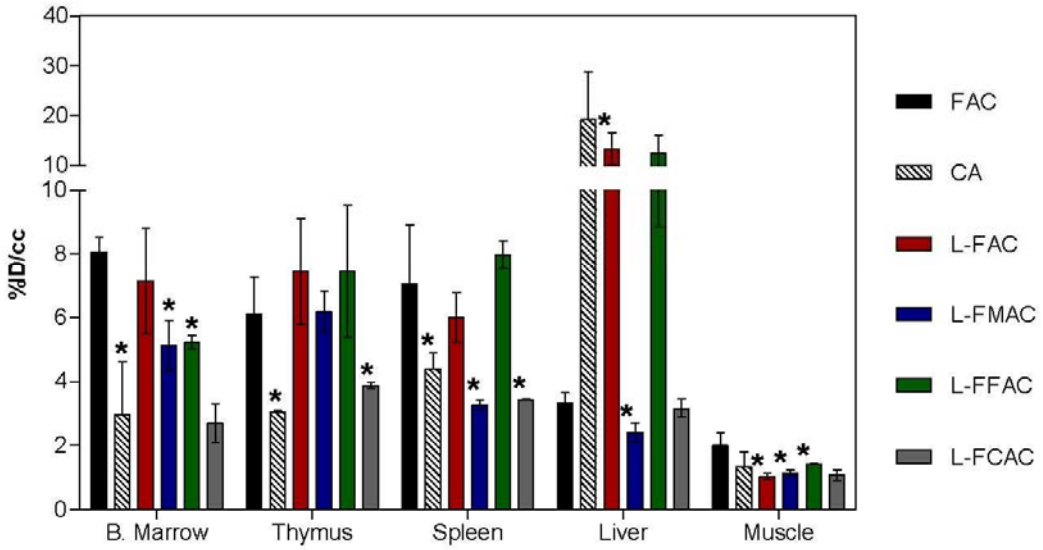

Supplemental Figure 6: **Quantification of microPET raw data shown in Figure 4**. The L-analog probes were injected intravenously into C57Bl/6 mice and images were acquired 60 min post injection (n≥3; mean with SD error bars). (*P* values are calculated relative to FAC for each specific tissue. * = $P<0.05$, n=5 (^{18}F-FAC), n=3 (L-^{18}F-FAC), n=3 (L-^{18}F-FMAC), n=2 (L-^{18}F-FFAC), n=2 (L-^{18}F-FCAC)).

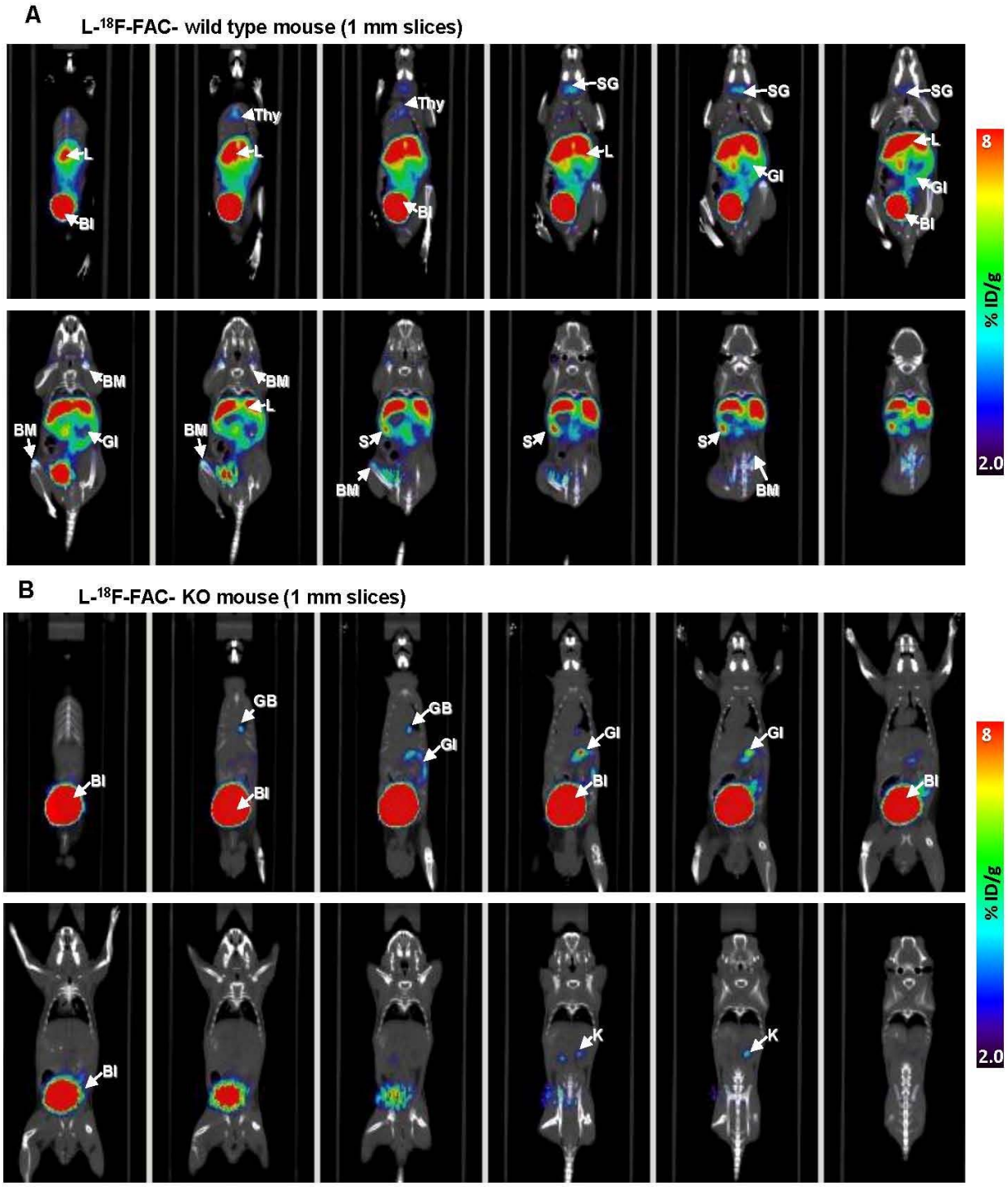

Supplemental Figure 7: Lack of *in vivo* uptake of ^{18}F-L-FAC in the dCK KO mice. 1-mm coronal slices of (**A**) WT and (**B**) dCK KO mice imaged 60 min post i.v. administration of 200 μCi of ^{18}F-L-FAC. Thy, thymus; BM, bone marrow; S, spleen; L, liver; GI, gastrointestinal tract; K, kidney; Bl, bladder.

References

1. Qi J, Leahy RM, Cherry SR, Chatziioannou A, Farquhar TH. High-resolution 3D Bayesian image reconstruction using the microPET small-animal scanner. *Phys Med Biol.* 1998;43:1001-1013.

2. Chow PL, Stout DB, Komisopoulou E, Chatziioannou AF. A method of image registration for small animal, multi-modality imaging. *Phys Med Biol.* 2006;51:379-390.

3. Loening AM, Gambhir SS. AMIDE: a free software tool for multimodality medical image analysis. *Mol Imaging.* 2003;2:131-137.

4. Pankiewicz KW, Krzeminski J, Ciszewski LA, Ren WY, Watanabe KA. A synthesis of 9-(2-deoxy-2-fluoro-.beta.-D-arabinofuranosyl)adenine and -hypoxanthine. An effect of C3'-endo to C2'-endo conformational shift on the reaction course of 2'-hydroxyl group with DAST. *The Journal of Organic Chemistry.* 2002;57:553-559.

5. Radu CG, Shu CJ, Nair-Gill E, et al. Molecular imaging of lymphoid organs and immune activation by positron emission tomography with a new [18F]-labeled 2'-deoxycytidine analog. *Nat Med.* 2008;14:783-788.

6. Radu CG, Witte ON, Nair-Gill ED, Satyamurthy N, Shu CJ, Czernin J; The Regents of the University of California assignee. Positron Emission Tomography Probes for Imaging Immune Activation and Selected Cancers. US Patent Application Publication No.: US 2009/0105184. April 23, 2009.